Electronic Supplementary Material (ESI) for Journal of Materials Chemistry C.

Supporting Information

Molecular Optimization of Incorporating Pyran Fused Acceptor-Donor-Acceptor Type Acceptors Enables over 15% Efficiency in Organic Solar Cells

Simin Wu[a], *Lingxian Meng*[a], *Zhe Zhang*[a], *Mingpeng Li*[a], *Yang Yang*[b], *Jian Wang*[b], *Hongbin Chen*[a], *Changzun Jiang*[a], *Xiangjian Wan*[a], *Chenxi Li*[a], *Zhaoyang Yao**[a], *Yongsheng Chen**[a]

[a]State Key Laboratory and Institute of Elemento-Organic Chemistry, The Centre of Nanoscale Science and Technology and Key Laboratory of Functional Polymer Materials, Renewable Energy Conversion and Storage Center (RECAST), College of Chemistry, Nankai University, Tianjin 300071, China

[b]The Institute of Seawater Desalination and Multipurpose Utilization, Ministry of Natural Resources (Tianjin), Tianjin 300192, China

E-mail: yschen99@nankai.edu.cn; zyao@nankai.edu.cn

Experimental Section

Materials and synthesis. All reactions and manipulations were carried out under argon atmosphere with the use of standard Schlenk techniques. All starting materials were purchased from commercial suppliers and used without further purification unless indicated otherwise. Polymer donor PM6 was purchased from Solarmer Material (Beijing) Inc. 3-Bromo-4-n-octylthiophene (compound 3) and 2,7-dibromo-3,6-dimethoxy-9,9-dioctyl-9H-fluorene (compound 7) were synthesized according to the literatures.[1, 2]

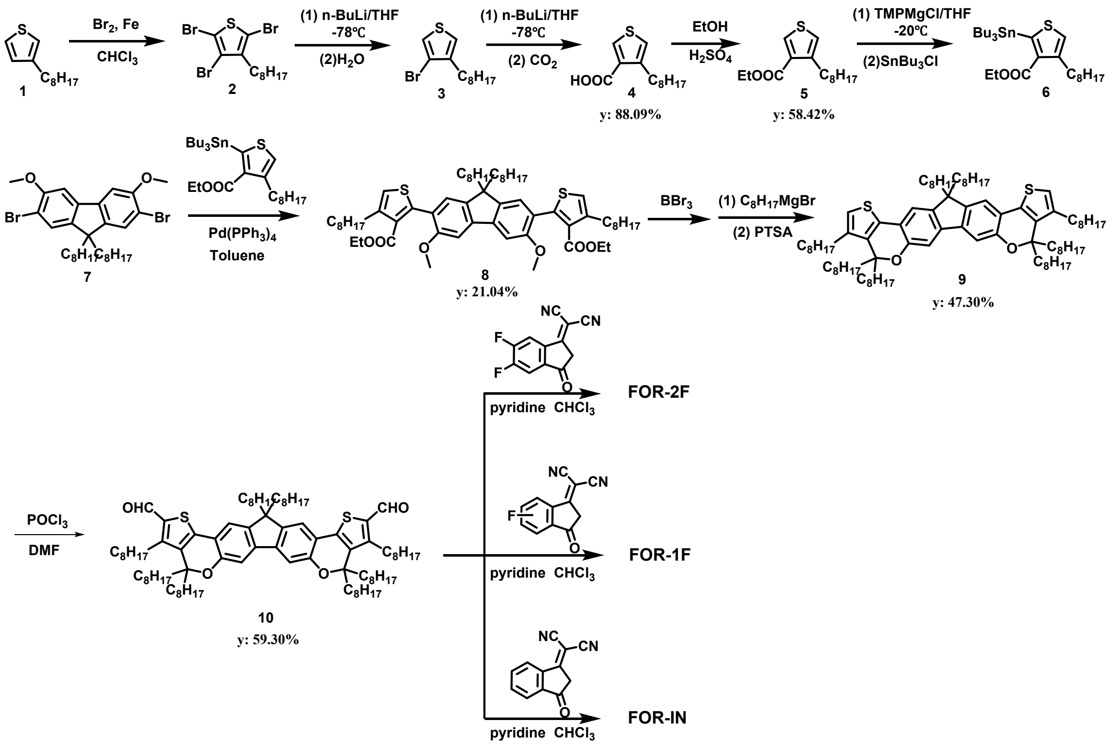

Scheme S1. Synthetic Route of FOR-2F, FOR-1F and FOR-IN.

Synthesis of Compound 4. Compound 3 (2.73 g, 9.92 mmol) was dissolved in 50 ml dry THF and the reaction mixture was cooled down to -78 °C. Then 6.82 ml *n*-BuLi (1.6 M solution in hexane) was added slowly, and the reaction mixture was stirred at -78 °C for half an hour. Then dry ice (4.36 g, 99.18 mmol) was added to the solution. After 4 h stirring, the reaction was quenched by water and extracted with CH_2Cl_2 (50 mL × 2). The combined organic layer was dried over anhydrous Na_2SO_4, the solvent was removed under reduced pressure to give **4** (2.10 g, 88%) as a dark oil which was used without further purification.

Synthesis of Compound 5. Compound 4 (2.10 g, 8.74 mmol) was dissolved in 50 ml dry EtOH, H_2SO_4 (1 ml) was added slowly, the mixture was heated to 80 °C for 12 h. After cooling to room temperature, the mixture was poured into water and then extracted with CH_2Cl_2 (50 mL × 2). The combined organic layer was dried over anhydrous Na_2SO_4, and the solvent was removed under vacuum, the crude product was purified by column chromatography (petroleum ether/CH_2Cl_2 2:1) to give colorless oil (1.37 g, 58%).

^1H NMR (400 MHz, $CDCl_3$): δ 8.06 (s, 1H), 6.90 (s, 1H), 4.29 (q, J = 6.9 Hz, 2H), 2.92 – 2.85 (t, 3H), 1.62 (m, J = 14.1, 7.0 Hz, 3H), 1.40 – 1.31 (m, 6H), 0.87 (m, J = 13.7, 5.9 Hz, 8H).

^{13}C NMR (101 MHz, CDCl3) δ 163.15, 144.22, 134.14, 131.74, 121.78, 60.26, 31.90, 30.19, 29.98, 29.57, 29.51, 29.32, 22.69, 14.33, 14.10.

Synthesis of Compound 6. Compound 5 (430 mg, 1.60 mmol) was dissolved in 50 ml dry THF and the reaction mixture was cooled down to -20 °C. Then 2.40 ml TMPMgCl (1 M solution in hexane) was added slowly, and the reaction mixture was stirred at -20 °C for 2 h. Then $SnBu_3Cl$ (0.84 ml, 2.88 mmol) was added to the solution. and the reaction mixture was stirred at room temperature for 3 h. After that, he mixture was poured into water and then extracted with CH_2Cl_2 (50 mL × 2). The combined organic layer was dried over anhydrous Na_2SO_4, the solvent was removed under reduced pressure to give **6** (0.84 g, 94%) as a dark oil which was used without further purification.

Synthesis of Compound 8. A solution of 2,7-dibromo-3,6-dimethoxy-9,9-dioctyl-9*H*-

fluorene (2 g, 3.29 mmol) and compound 6 (5.50 g, 9.86 mmol) in 100 mL DMF and was degassed twice with argon. Then $Pd(PPh_3)_4$ (0.19 g, 0.16 mmol) was added and the mixture was stirred at 120 °C for 24 h under argon, after which the mixture was poured into water (100 mL), and extracted with dichloromethane (100 mL × 2). The organic layer was then dried over anhydrous Na_2SO_4. The solvent was removed and the crude product was purified by column chromatography to obtain a yellow oil (0.68 g, 21%).

^1H NMR (400 MHz, $CDCl_3$): δ 7.27 (s, 2H), 7.21 (s, 2H), 6.94 (s, 2H), 4.08 (q, J = 7.1 Hz, 4H), 3.87 (s, 6H), 2.88 – 2.80 (t, 6H), 1.98 – 1.83 (m, 4H), 1.66 (d, J = 14.9 Hz, 8H), 1.39 – 1.21 (m, 24H), 0.99 (m, J = 5.5 Hz, 10H), 0.86 (m, J = 9.9, 7.6, 3.7 Hz, 24H).

^{13}C NMR (101 MHz, $CDCl_3$): δ 165.14, 156.04, 145.01, 143.95, 143.34, 142.01, 130.37, 124.92, 123.11, 119.99, 101.73, 60.06, 55.59, 54.35, 40.21, 31.95, 31.85, 31.64, 30.17, 30.13, 30.03, 29.68, 29.54, 29.36, 29.34, 29.25, 22.73, 22.66, 22.62, 14.12, 14.07.

Synthesis of Compound 9. Compound 8 (0.68 g, 0.69 mmol) was dissolved in 50 mL dry CH_2Cl_2 and the reaction mixture was cooled down to -78 °C. Then 3.46 mL BBr_3 (1.0 M solution in CH_2Cl_2) was added slowly, and the reaction mixture was stirred at room temperature for 12 h. After that, the reaction was quenched by water and extracted with CH_2Cl_2. After dried over anhydrous Na_2SO_4, the precipitation was dissolved in 50 mL dry THF and 3.5 mL octyl-magnesium bromide (2.0 M solution in diethyl ether) was added at -78 °C. Then the reaction was stirred at room temperature for 12 h, and the mixture was extracted with CH_2Cl_2 (100 mL × 3). The organic layer was dried over anhydrous Na_2SO_4, and after removal of the solvent, the crude product was dissolved in 50 mL toluene, and reacted with p-toluene sulfonic acid (0.28 g, 1.45 mmol) at 110°C for 12 h. The mixture was extracted with CH_2Cl_2 and water, dried over anhydrous Na_2SO_4, and was purified by silica gel chromatography using petroleum ether as eluent, yielding a solid product 9 (0.42 g, 47%).

^{1}H NMR (400 MHz, $CDCl_3$) δ 7.11 (s, 2H), 7.04 (s, 2H), 6.84 (s, 2H), 2.56 – 2.46 (m, 4H), 2.05 – 1.76 (t, 14H), 1.76 – 1.66 (m, 4H), 1.43 (m, 18H), 1.33 – 1.11 (m, 38H), 0.83 (m, 34H).

^{13}C NMR (101 MHz, $CDCl_3$) δ 151.24, 143.66, 141.51, 140.07, 135.13, 134.14, 125.54, 118.34, 118.29, 116.18, 106.96, 85.80, 54.04, 40.68, 40.39, 32.26, 31.98, 31.91, 30.36, 30.09, 30.00, 29.86, 29.79, 29.65, 29.56, 29.35, 29.03, 24.03, 23.81, 22.75, 22.71, 14.45, 14.12.

Synthesis of Compound 10. $POCl_3$ (0.22 mL) was added drop by drop to DMF (2 mL) at 0°C under the protection of argon and then stirred at room temperature for 5 h to gain the Vilsmerier reagent. The Vilsmerier reagent was added into a 1,2-dichloroethane (50 mL) solution of compound 9 (0.42 g, 0.33 mmol). The above reaction mixture was stirred at room atmosphere for 1 h and then heated to 80 °C for 12 h. The mixture was quenched with CH_3COONa (aq.), and then extracted with CH_2Cl_2 (50 mL × 2). The combined organic layer was dried over anhydrous Na_2SO_4 and purified by silica gel, yielding a yellow solid (0.26 g, 59%).

^{1}H NMR (400 MHz, CDCl3) δ 10.02 (s, 2H), 7.23 (s, 2H), 7.07 (s, 2H), 2.94 – 2.84 (t , 4H), 2.05 – 1.82 (m, 12H), 1.56 (d, J = 73.4 Hz, 14H), 1.26 (dd, J = 24.8, 12.3 Hz, 74H), 0.94 – 0.69 (m, 32H).

^{13}C NMR (101 MHz, CDCl3) δ 180.56, 151.54, 148.60, 143.36, 142.73, 142.58, 135.08, 135.04, 116.47, 116.00, 106.39, 84.60, 53.13, 40.22, 39.35, 32.13, 30.92, 30.83, 30.78, 30.49, 30.41, 29.23, 29.18, 29.12, 28.86, 28.79, 28.69, 28.43, 28.32, 28.23, 28.19, 28.17, 27.08, 23.00, 22.82, 21.63, 21.61, 13.07, 13.05.

MS (MALDI-TOF): calcd for $C_{89}H_{142}O_4S_2$ [M$^+$] 1340.23; found: 1340.40.

Synthesis of Compound FOR-IN. Under the protection of argon, compound 10 (100 mg, 0.08 mmol) and 3-(Dicyanomethylidene)indan-1-one (144.9 mg, 0.80 mmol) was dissolved in dry chloroform (50 mL), followed by the addition of pyridine (0.5 mL). After stirring at room temperature for 12 h, the mixture was poured into water and then extracted with $CHCl_3$ (50 mL × 2). The organic layer was dried over anhydrous Na_2SO_4 for 3 h. After removal of solvent, the crude product was purified by silica gel, and then recrystallized from $CHCl_3$ and methanol to give FOR-IN as a dark blue solid (105 mg, 83%).

^{1}H NMR (400 MHz, $CDCl_3$) δ 9.03 (s, 2H), 8.73 (d, J = 7.7 Hz, 2H), 7.96 (d, J = 5.5 Hz, 2H), 7.77 (m, 4H), 7.47 (s, 2H), 7.11 (s, 2H), 3.02 – 2.91 (m, 4H), 2.02 (d, J = 11.7 Hz, 12H), 1.56 (s, 14H), 1.18 (dd, J = 58.0, 28.1 Hz, 74H), 0.95 – 0.66 (m, 32H).

^{13}C NMR (101 MHz, $CDCl_3$): δ 188.73, 161.39, 156.94, 153.79, 150.25, 144.98, 140.00, 136.94, 136.53, 135.00, 134.56, 134.28, 131.56, 125.22, 123.50, 120.53, 118.23, 117.29, 115.37, 115.05, 107.65, 86.17, 77.32, 77.21, 77.01, 76.69, 68.01, 54.68, 41.54, 40.66, 33.27, 31.86, 31.78, 30.50, 29.90, 29.77, 29.49, 29.44, 29.31, 29.25, 24.07, 23.90, 22.68, 22.62, 14.12, 14.07.

MS (MALDI-TOF): calcd for $C_{113}H_{150}N_4O_4S_2$ [M^+] 1692.59; found: 1692.11.

Synthesis of Compound FOR-1F. Under the protection of argon, compound 10 (100 mg, 0.08 mmol) and 2-(5 or 6-fluoro-3-oxo-2,3-dihydro-1H-inden-1-ylidene)malononitrile (158.3 mg, 0.80 mmol) was dissolved in dry chloroform (50 mL), followed by the addition of pyridine (0.5 mL). After stirring at room temperature for 12 h, the mixture was poured into water and then extracted with $CHCl_3$ (50 mL × 2). The organic layer was dried over anhydrous Na_2SO_4 for 3 h. After removal of solvent, the crude product was purified by silica gel, and then recrystallized from $CHCl_3$ and methanol to give FOR-1F as a dark blue solid (110 mg, 85%).

^{1}H NMR (400 MHz, $CDCl_3$): δ 8.99 (s, 2H), 8.72 (m, 0.58H), 8.40 (d, 1.58H), 7.94 (m, 1.52H), 7.57 (d, 0.6H), 7.44 (s, 2H), 7.40 (d, 1.47H), 7.09 (s, 2H), 2.94 (t, 4H), 1.98 (t, 12H), 1.62 – 1.38 (m, 14H), 1.36 – 1.01 (m, 74H), 0.95 – 0.68 (m, 32H).

^{13}C NMR (101 MHz, $CDCl_3$): δ 187.27, 167.96, 165.40, 159.89, 157.35, 153.85, 150.91, 145.13, 145.04, 142.19, 136.61, 134.60, 133.04, 131.54, 121.68, 120.29, 118.28, 117.29, 115.08, 114.61, 112.89, 107.74, 86.21, 68.69, 54.69, 41.52, 40.63, 33.30, 31.85, 31.78, 30.51, 29.89, 29.76, 29.48, 29.44, 29.30, 29.25, 29.15, 24.07, 23.90, 22.67, 22.65, 22.62, 22.59, 14.12, 14.09, 14.07, 14.04.

MS (MALDI-TOF): calcd for $C_{113}H_{148}F_2N_4O_4S_2$ [M^+] 1728.57; found: 1728.09.

Synthesis of Compound FOR-2F. Under the protection of argon, compound 10 (100 mg, 0.08 mmol) and 2-(5,6-difluoro-3-oxo-2,3-dihydro-1H-inden-1-ylidene)malononitrile (171 mg, 0.80 mmol) was dissolved in dry chloroform (50 mL), followed by the addition of pyridine (0.5 mL). After stirring at room temperature for 12 h, the mixture was poured into water and then extracted with $CHCl_3$ (50 mL × 2). The organic layer was dried over anhydrous Na_2SO_4 for 3 h. After removal of solvent, the crude product was purified by silica gel, and then recrystallized from $CHCl_3$ and methanol to give FOR-2F as a dark blue solid (101 mg, 77%).

^{1}H NMR (400 MHz, $CDCl_3$): δ 9.03 (s, 2H), 8.60 (dd, J = 10.0, 6.5 Hz, 2H), 7.74 (t, J = 7.5 Hz, 2H), 7.51 (s, J = 24.5 Hz, 2H), 7.08 (s, J = 48.2 Hz, 2H), 2.98 (t, 4H), 2.29 – 1.99 (m, 12H), 1.70 – 1.46 (m, 14H), 1.49 – 1.05 (m, 74H), 1.01 – 0.54 (m, 34H).

^{13}C NMR (101 MHz, $CDCl_3$): δ 186.30, 159.20, 157.76, 153.94, 145.26, 145.11, 136.74, 134.62, 134.48, 131.53, 119.58, 118.32, 114.92, 114.62, 107.81, 86.24, 68.48, 54.69, 41.51, 40.60, 33.35, 31.85, 31.79, 31.78, 30.50, 29.87, 29.74, 29.48, 29.44, 29.30, 29.25, 24.07, 23.90, 22.67, 22.62, 14.12, 14.07.

MS (MALDI-TOF): calcd for $C_{113}H_{146}F_4N_4O_4S_2$ [M^+] 1764.55; found: 1764.08.

Measurements and Instruments. The ^{1}H and ^{13}C nuclear magnetic resonance (NMR) spectra were taken on a Bruker AV400 Spectrometer. Matrix assisted laser desorption/ionization time-of-flight (MALDI-TOF) mass spectrometry were performed on a Bruker Autoflex III instrument. Varian 7.0T FTMS was used to achieve the HR-MS data. UV-vis spectra were obtained with a Cary 5000 Spectrophotometers. Cyclic voltammogram (CV) was performed with a LK2010 Microcomputerbased Electrochemical Analyzer by using a three-electrode electrolytic cell with a film working electrode, a platinum counter electrode, and a calomel reference electrode. In a solution of acetonitrile using tetrabutylammonium hexafluorophosphate (Bu_4NPF_6) as the electrolyte, a low potential sweep rate of 100 mV s^{-1} was used and the electrochemically reversible ferrocene (Fc) was employed as internal reference during our CV measurements.Thermogravimetric analyses (TGA) were carried out on a NETZSCH STA 449 F5 Jupiter instrument under a purified nitrogen gas. The heating rate is a 10 °C min^{-1} heating rate. The current density-voltage (J-V) curves of photovoltaic devices were obtained by a Keithley 2400 source-measure unit. The photocurrent was measured under simulated illumination of 100 mW cm^{-2} with AM1.5G irradiation using a xenon-lamp-based solar simulator [Oriel 96000] in an argon-filled glove box. External quantum efficiency values (EQEs) of the encapsulated devices were obtained with a halogen-tungsten lamp, monochromator, optical chopper, and lock-in amplifier in air and the photon flux was determined by a calibrated silicon photodiode. Atomic force microscopy (AFM) images were performed using in tapping mode on a Bruker MutiMode 8 atomic force microscope. The GIWAXS (grazing incidence wide angle X-ray scattering) samples were prepared on ZnO-coated Si substrates using the same preparation conditions as for devices. SCLC was uesd to measure hole and electron mobilities, using a diode configuration of ITO/PEDOT:PSS/active layer/Au for hole and glass/ZnO/active layer/Al for electron by taking the dark current density in the range of 0–8 V and fitting the results to a space charge limited form.

Fabrication of OPV devices. The photovoltaic devices were fabricated with a structure of indium tinoxide (ITO)/ZnO/PFN-Br/ donor:acceptor /MoOx/Ag. The ITO-coated glass substrates were cleaned by ultrasonic treatment in detergent, deionized water, acetone, and isopropyl alcohol under ultrasonication for 15 minutes each time and subsequently dried by a nitrogen flow. A 30 nm thick layer of ZnO precursor solution was spin-coated (3000 rpm) onto the ITO surface. After baked at 200 °C for 60 min, the substrates were transferred into an argon-filled glove box. A thin film of PFN-Br was spin-coated on ZnO. Subsequently, the active layer was spin-coated from blend chlorobenzene solutions and then MoOx (~6 nm) and Ag (~70 nm) was successively evaporated onto the active layer through a shadow mask.

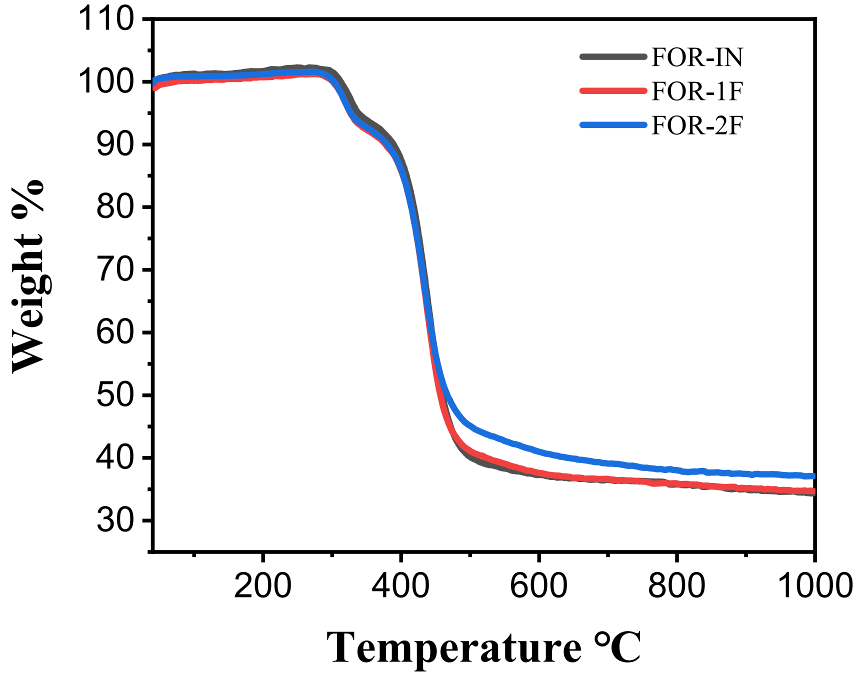

Fig. S1 TGA curves of FOR-IN, FOR-1F and FOR-2F with a heating rate of 10 °C/min under N_2 atmosphere.

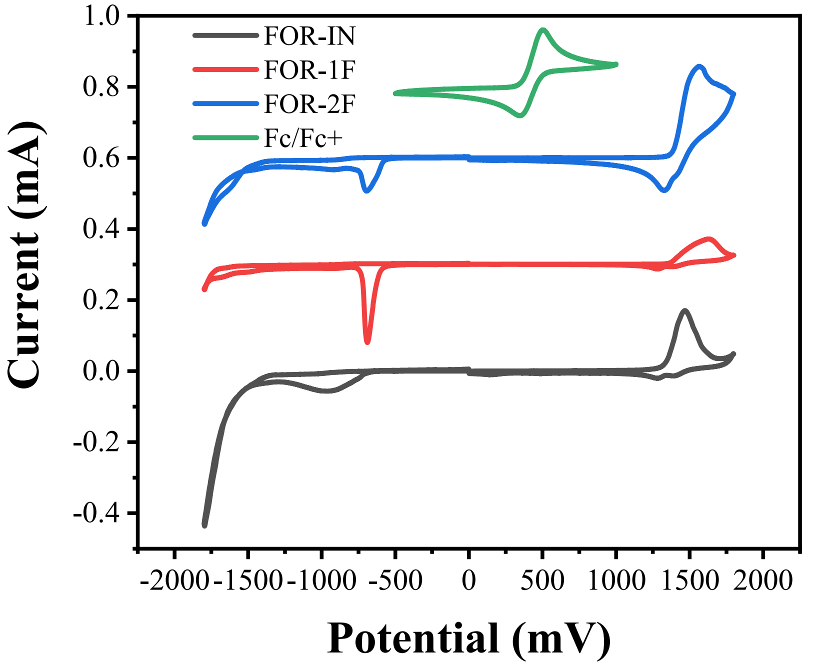

Fig. S2 Cyclic voltammogram of FOR-IN, FOR-1F, FOR-2F and Fc/Fc^+ in acetonitrile solution with 0.1 mol L^{-1} n-Bu_4NPF_6 at a scan rate of 100 mV s^{-1}

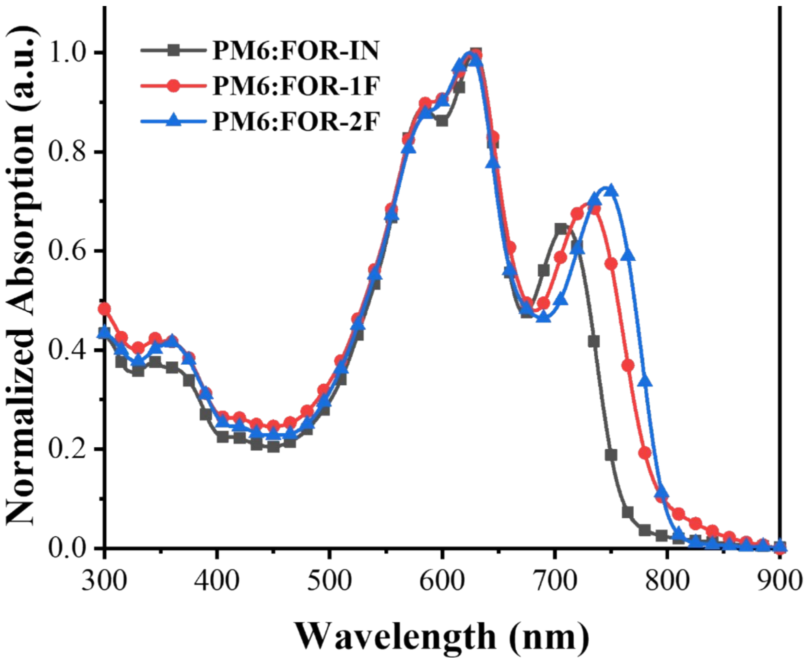

Fig. S3 The absorption spectra of PM6:FOR-IN, PM6:FOR-1F and PM6:FOR-2F blend films.

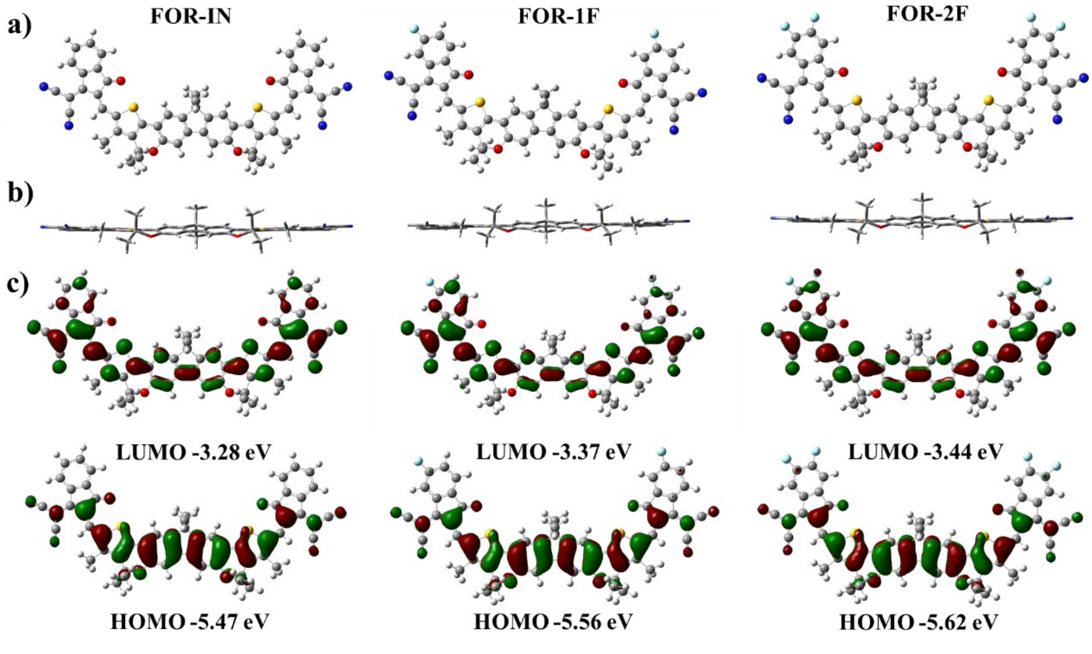

Fig. S4 The optimized geometries for FOR-IN, FOR-1F and FOR-2F from (a) top view and (b) side view. (c) Theoretical density distribution for the frontier molecular orbits of FOR-IN, FOR-1F and FOR-2F. All calculations were carried out using Gaussian 16

Table S1. Performance of the OSCs with different PM6 (D)/ FOR-IN (A) ratios.

D:A	V_{OC} (V)	*FF* (%)	J_{SC}(mA/cm^2)	PCE (%)
1:0.8	1.111	51.84	13.05	7.52
1:1	1.105	52.82	13.31	7.77

1:1.2	1.104	52.18	12.51	7.20

Table S2. Photovoltaic performance of solar cells based on PM6:FOR-IN (1:1, w/w) blend films with different TA temperature.

TA (°C)	V_{OC} (V)	FF (%)	J_{SC}(mA/cm^2)	PCE (%)
none	1.111	51.84	13.05	7.52
120	1.071	57.98	15.38	9.55
140	1.073	55.72	14.68	8.78

Table S3. Performance of the OSCs based on PM6:FOR-IN (1:1, w/w) blend films with different additives.

Additves	V_{OC} (V)	FF (%)	J_{SC}(mA/cm^2)	PCE (%)
none	1.071	57.98	15.38	9.55
DIO	1.060	55.25	15.08	8.83
CN	1.040	57.30	13.80	8.21

Table S4. Performance of the OSCs with different PM6 (D)/ FOR-1F (A) ratios.

D:A	V_{OC} (V)	FF (%)	J_{SC}(mA/cm^2)	PCE (%)
1:0.8	1.037	57.38	16.59	9.87
1:1	1.034	59.04	16.90	10.32
1:1.2	1.030	58.42	17.05	10.26

Table S5. Photovoltaic performance of the solar cells based on PM6:FOR-1F (1:1, w/w) blend films with different TA temperature.

TA (°C)	V_{OC} (V)	FF (%)	J_{SC}(mA/cm^2)	PCE (%)
none	1.034	59.04	16.90	10.32
120	1.007	59.20	18.97	11.31
140	1.012	62.10	18.84	11.84
160	1.002	60.50	18.33	11.13

Table S6. Performance of the OSCs based on PM6:FOR-1F (1:1, w/w) blend films with different additives.

Additive	V_{OC} (V)	FF (%)	J_{SC}(mA/cm^2)	PCE (%)
none	1.034	59.04	16.90	10.32
DIO	1.013	63.00	18.99	12.13

CN	1.009	63.50	18.38	11.78

Table S7. Performance of the OSCs based on PM6:FOR-1F (1:1, w/w) blend films with different DIO ratios.

Additive(v/v)	V_{OC} (V)	FF (%)	J_{SC}(mA/cm2)	PCE (%)
0.3	1.013	63.00	18.99	12.13
0.5	1.020	66.21	18.65	12.59
0.7	1.010	62.30	18.01	11.33

Table S8. Performance of the OSCs with different PM6 (D)/ FOR-2F (A) ratios.

D:A	V_{OC} (V)	FF (%)	J_{SC}(mA/cm^2)	PCE (%)
1:0.8	0.997	65.27	18.16	11.81
1:1	0.994	65.25	18.84	12.22
1:1.2	0.976	61.82	18.51	11.17

Table S9. Photovoltaic performance of the solar cells based on PM6:FOR-2F (1:1, w/w) blend films with different TA temperature.

TA (°C)	V_{OC} (V)	FF (%)	J_{SC}(mA/cm^2)	PCE (%)
none	0.994	65.25	18.84	12.22
120	0.968	70.00	20.34	13.79
140	0.971	71.60	20.84	14.49
160	0.961	70.20	20.65	13.92

Table S10. Performance of the OSCs based on PM6:FOR-2F (1:1, w/w) blend films with different additives.

Additive	V_{OC} (V)	FF (%)	J_{SC}(mA/cm^2)	PCE (%)
none	1.034	59.04	16.90	10.32
DIO	0.969	73.47	21.25	15.18
CN	0.968	71.60	21.12	14.65

Table S11. Performance of the OSCs based on PM6:FOR-2F (1:1, w/w) blend films with different DIO ratios.

Additive(v/v)	V_{OC} (V)	FF (%)	J_{SC}(mA/cm^2)	PCE (%)
0.1	0.969	72.46	20.48	14.39

0.3	0.969	73.47	21.25	15.18
0.5	0.972	72.40	20.65	14.54
0.7	0.973	71.30	20.68	14.35

Table S12. Summary of the GIWAXS parameters for PM6:FOR-IN, PM6:FOR-1F and PM6:FOR-2F films.

blends		out-of-plane			
		q(Å^{-1})	d(Å)	Fwfm(Å^{-1})	CCL(Å)
PM6:FOR-IN	(010) stacking	1.74	3.61	0.193	29.34
PM6:FOR-1F	(010) packing	1.74	3.61	0.170	33.31
PM6:FOR-2F	(010) stacking	1.71	3.67	0.137	41.23

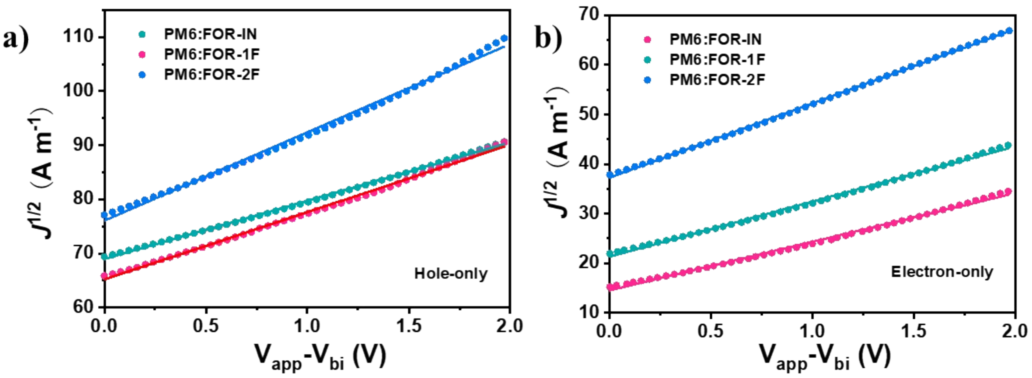

Fig. S5 Hole-only (a) and electron-only (b) devices based on PM6:FOR-IN, PM6:FOR-1F and PM6:FOR-2F devices, respectively. The solid lines represent the fit using a model of single carrier SCLC with field-independent mobility. The J_D-V characteristic are corrected for the built-in voltage V_{bi} that arises the work function difference between the contacts.

Table S13. Hole mobilities and electron mobilities of four blends

	μ_h	μ_e	μ_h/μ_e
PM6:FOR-IN	6.71×10^{-5}	5.55×10^{-5}	1.21
PM6:FOR-1F	8.99×10^{-5}	7.12×10^{-5}	1.26
PM6:FOR-2F	1.54×10^{-4}	1.30×10^{-4}	1.18

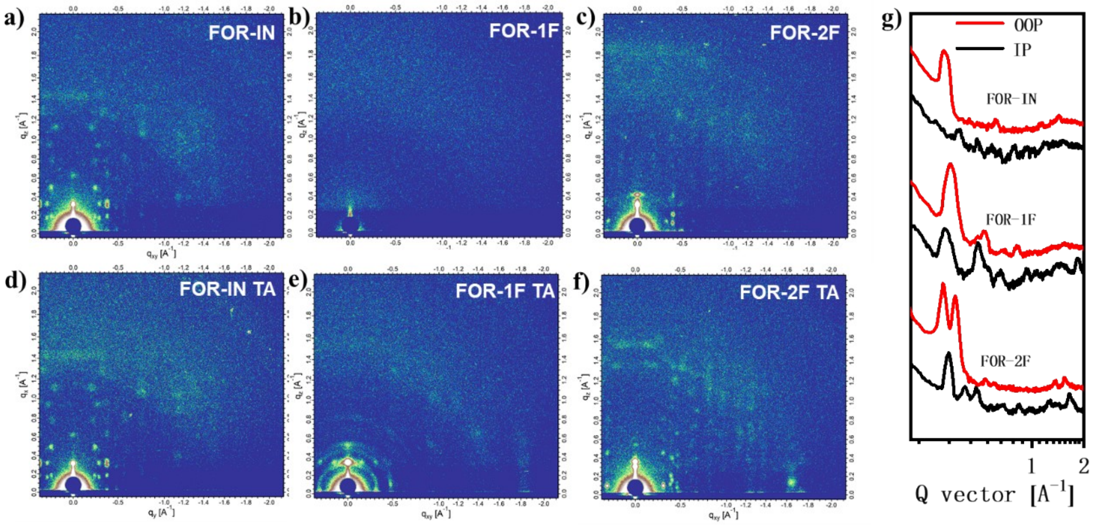

Fig. S6 GIWAXS pattern for (a) FOR-IN pristine film, (b) FOR-1F pristine film, (c) FOR-2F pristine film, (d) FOR-IN film after TA (e) FOR-1F film after TA, (f) FOR-2F film after TA. (g) In-plane and Out-of -plane line cuts of the GIWAXS patterns for the corresponding pure films after TA.

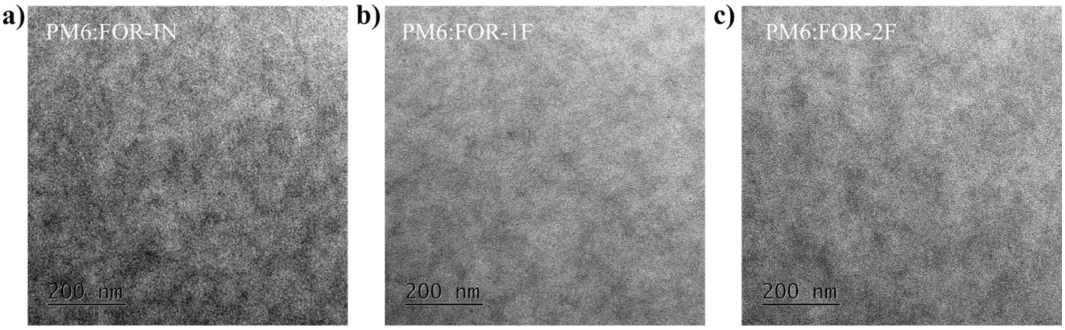

Fig. S7 The TEM images of a) PM6:FOR-IN, b) PM6:FOR-1F, c) PM6:FOR-2F blend films.

NMR and MS spectra

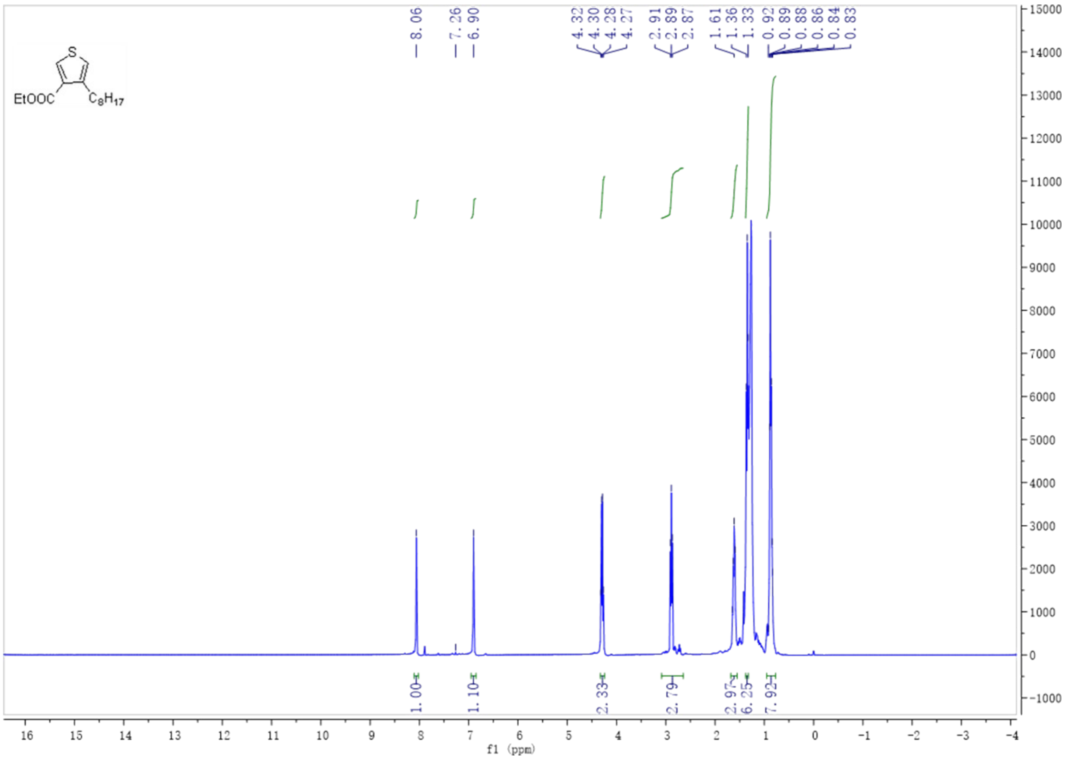

Fig. S8 ^{1}H NMR spectra of Compound 5 in $CHCl_3$

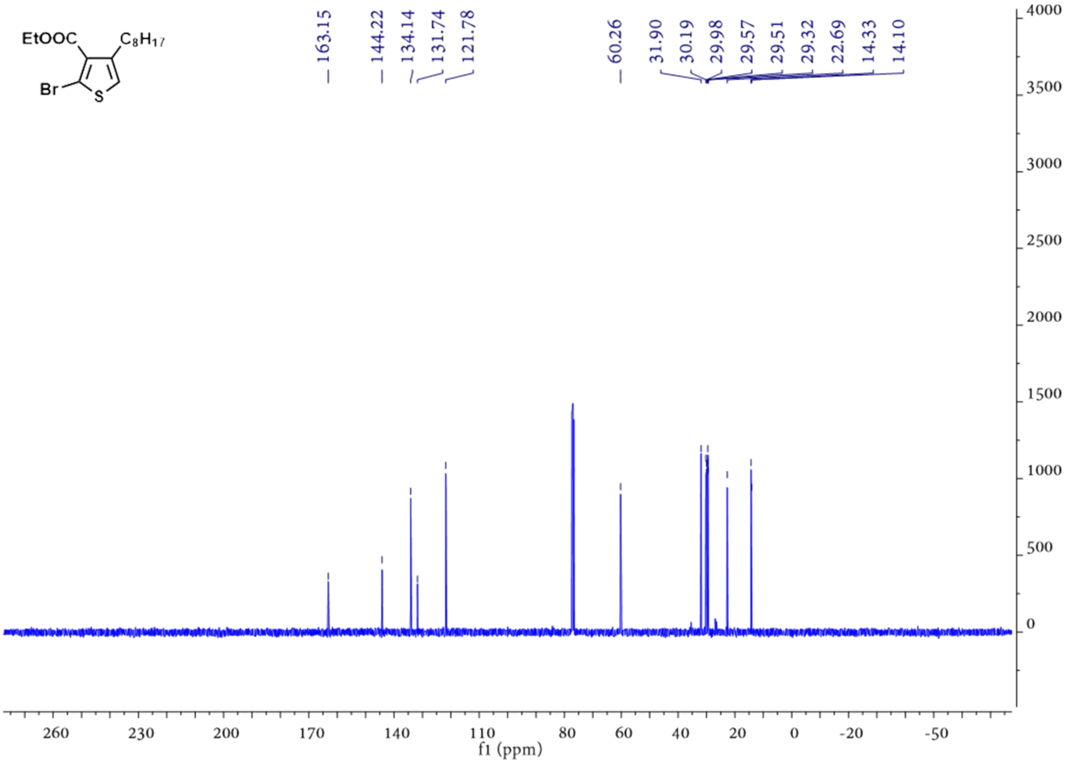

Fig. S9 ^{13}C NMR spectra of Compound 5 in $CHCl_3$

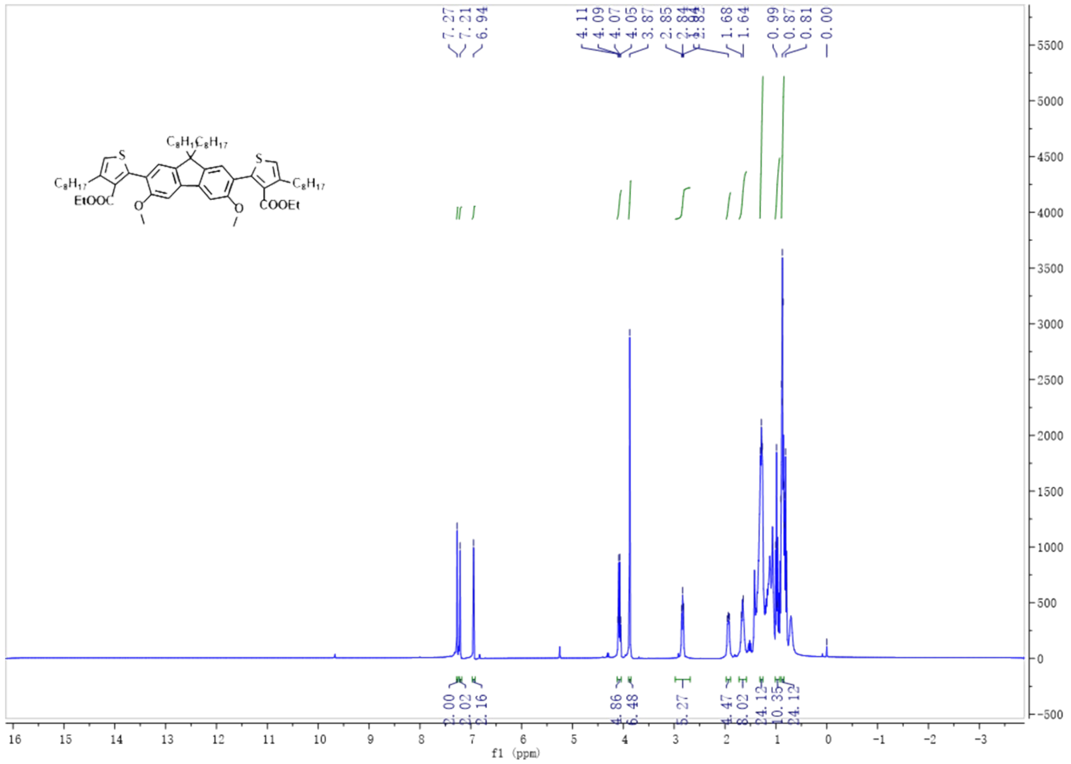

Fig. S10 ^{1}H NMR spectra of Compound 8 in $CHCl_3$

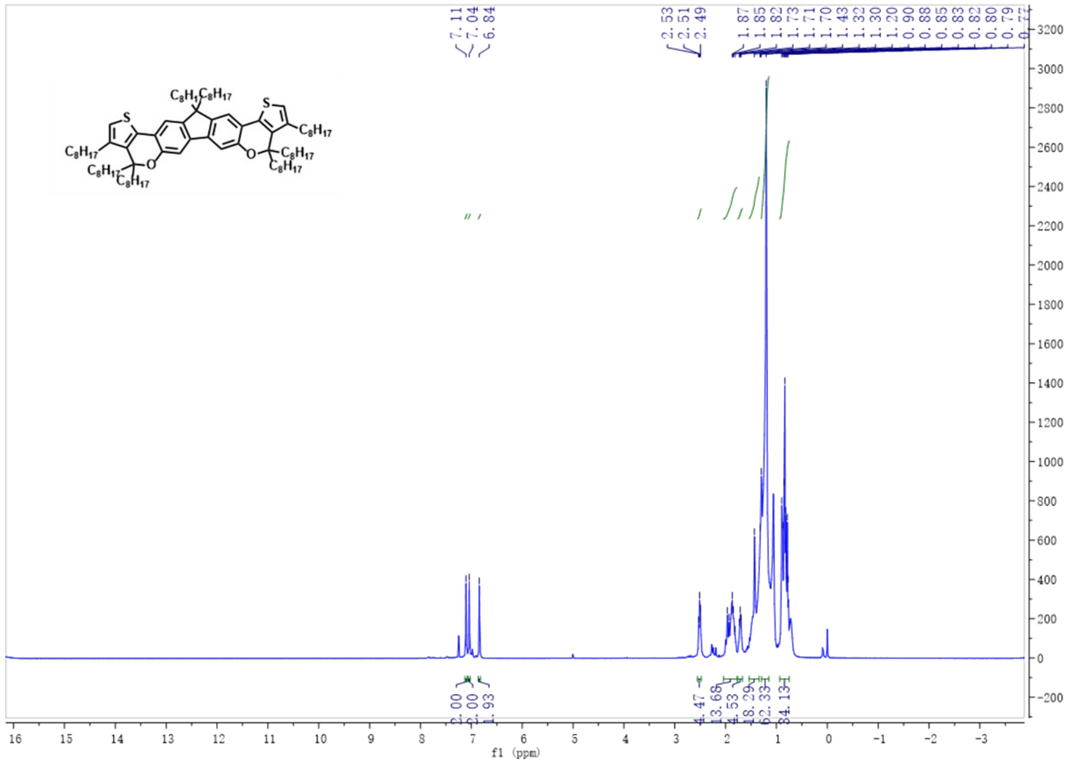

Fig. S11 ^{1}H NMR spectra of Compound 9 in $CHCl_3$

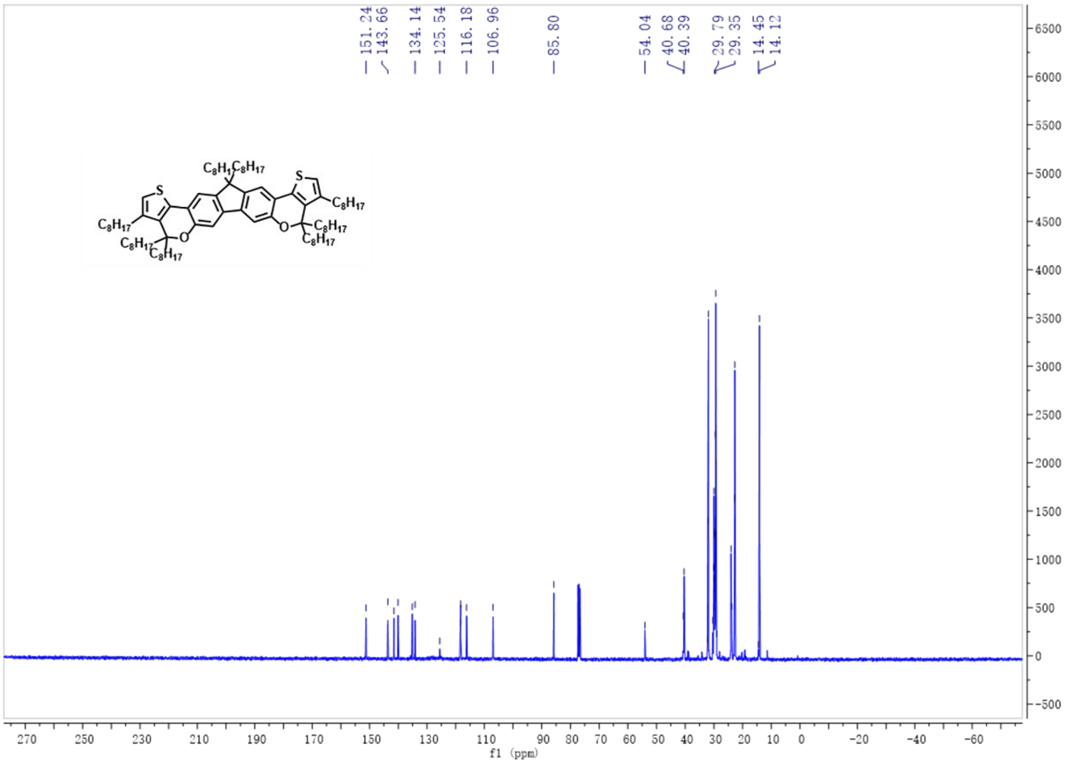

Fig. S12 ^{13}C NMR spectra of Compound 9 in $CHCl_3$

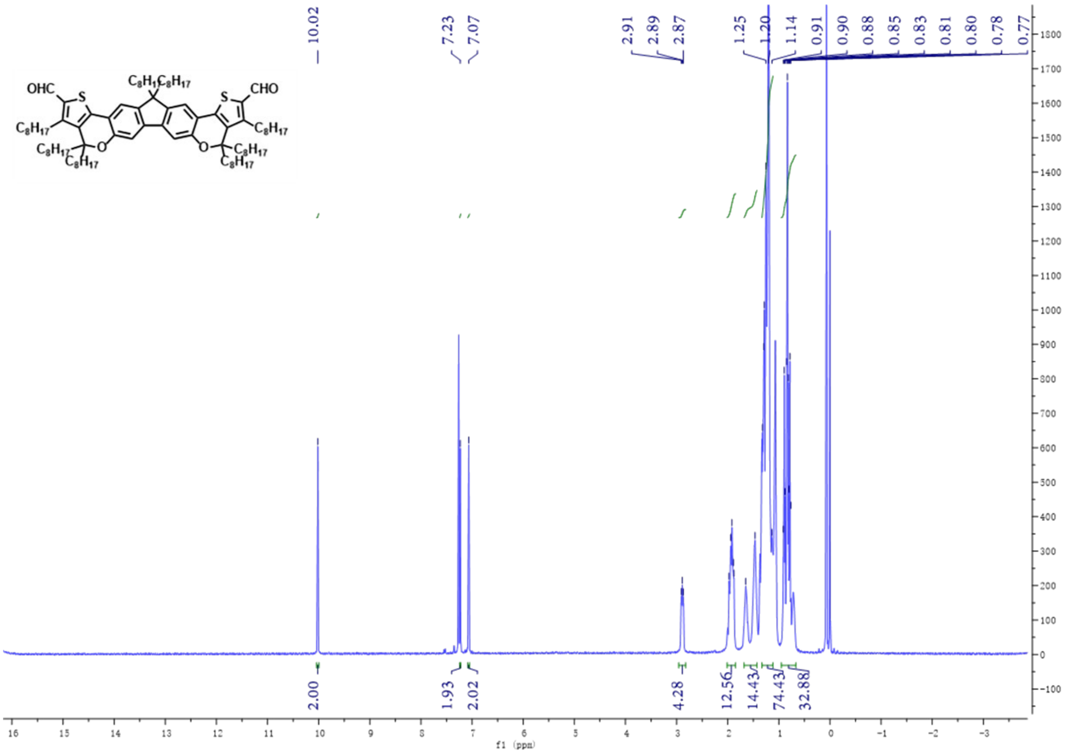

Fig. S13 ^{1}H NMR spectra of Compound 10 in $CHCl_3$

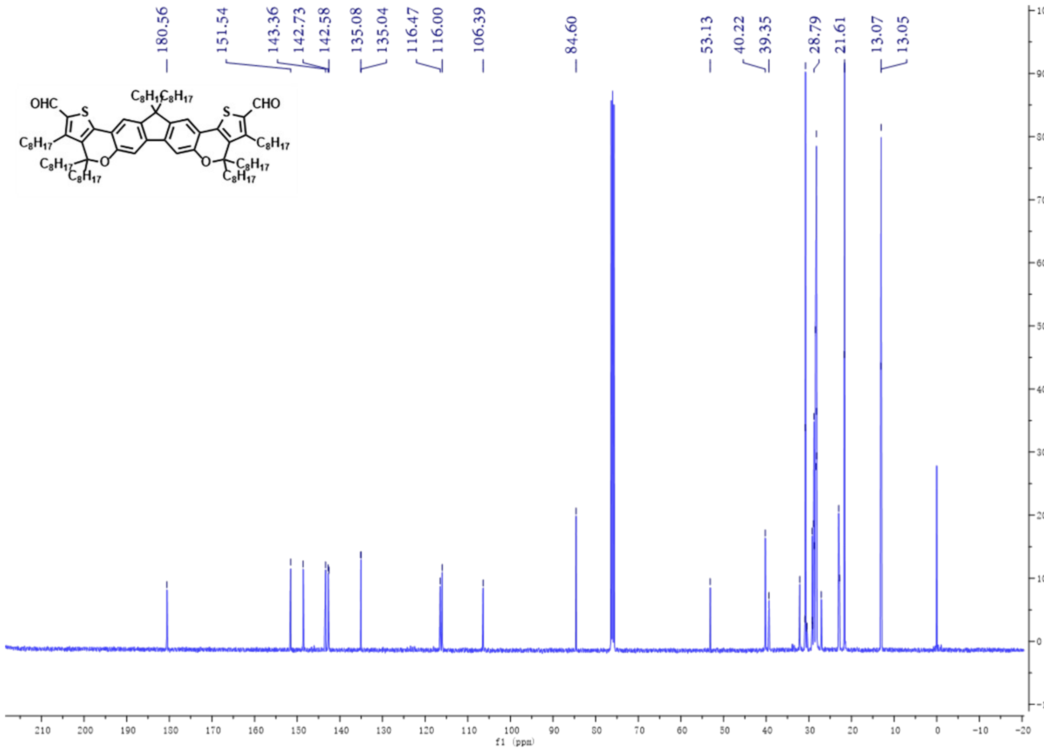

Fig. S14 ^{13}C NMR spectra of Compound 10 in $CHCl_3$

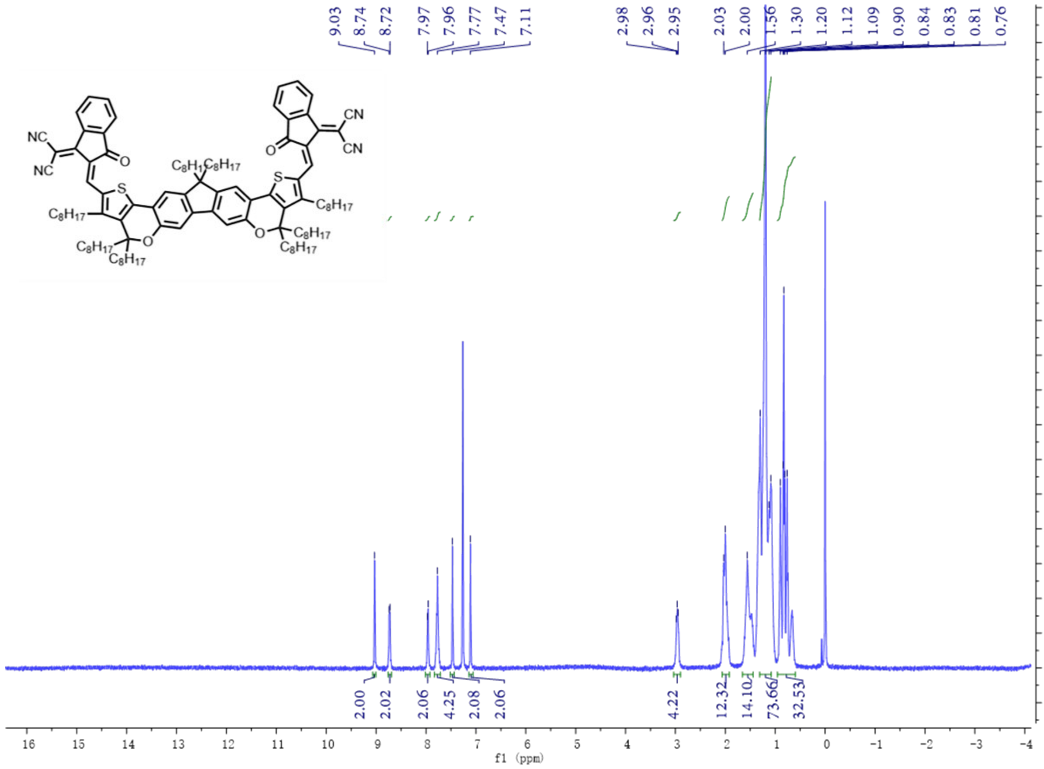

Fig. S15 ^{1}H NMR spectra of compound FOR-IN in $CHCl_3$

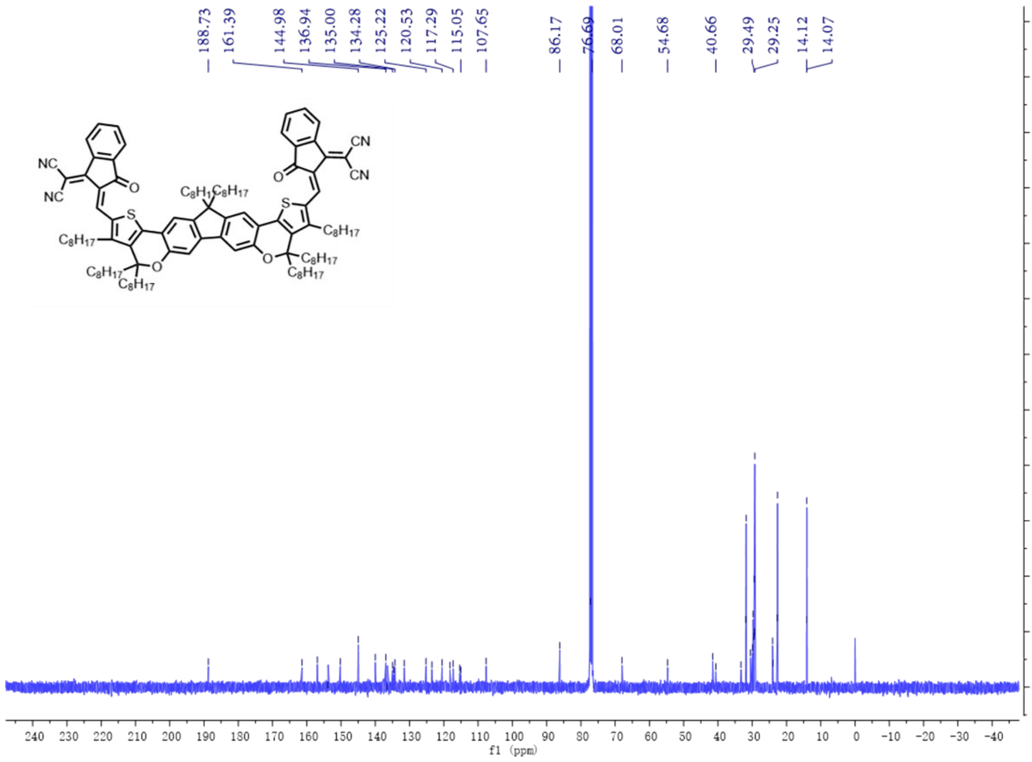

Fig. S16 ^{13}C NMR spectra of compound FOR-IN in $CHCl_3$

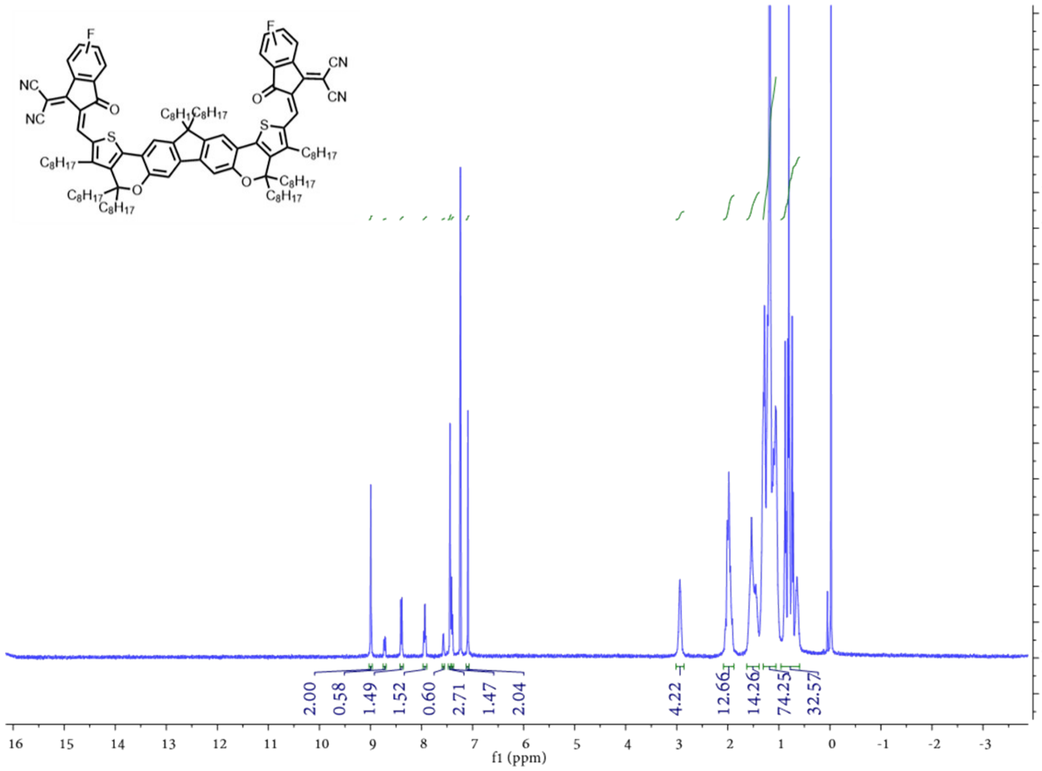

Fig. S17 ^{1}H NMR spectra of compound FOR-1F in $CHCl_3$

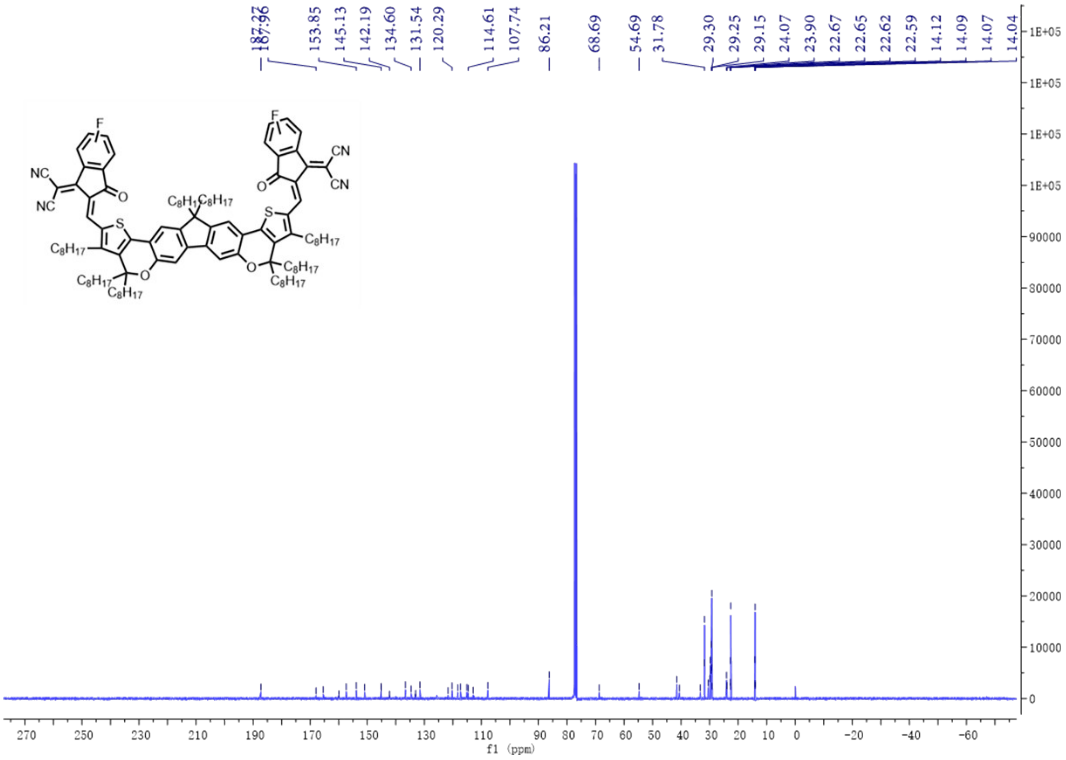

Fig. S18 ^{13}C NMR spectra of compound FOR-1F in $CHCl_3$

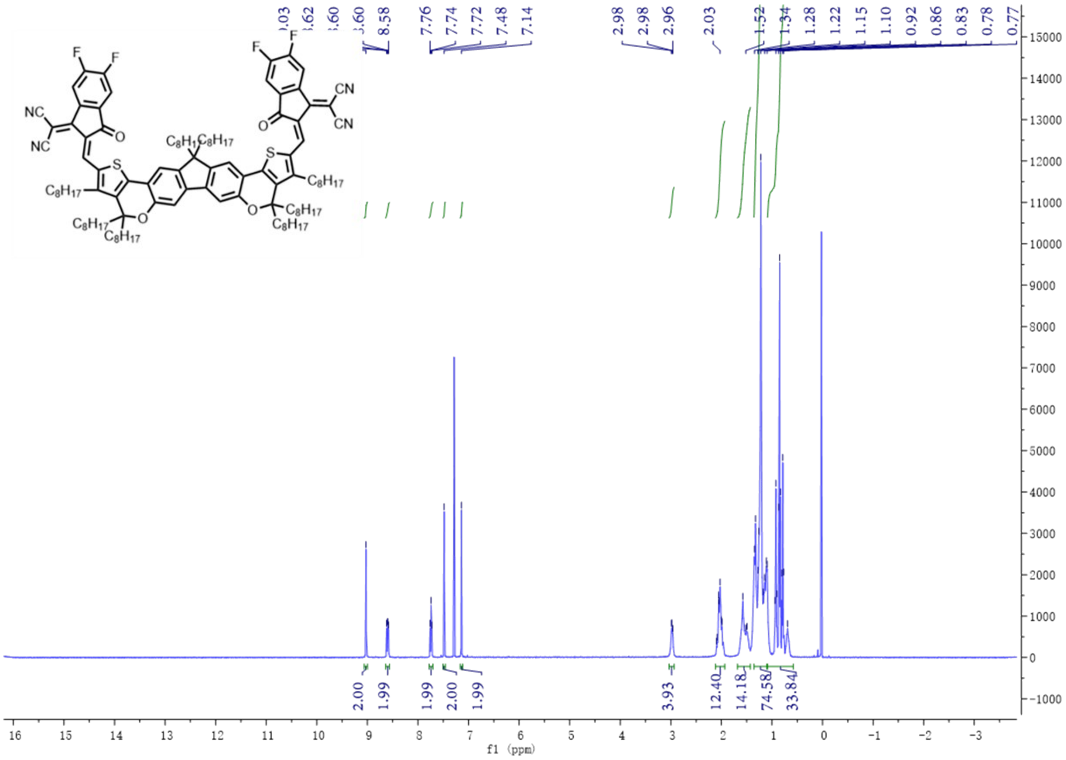

Fig. S19 ^{1}H NMR spectra of compound FOR-2F in $CHCl_3$

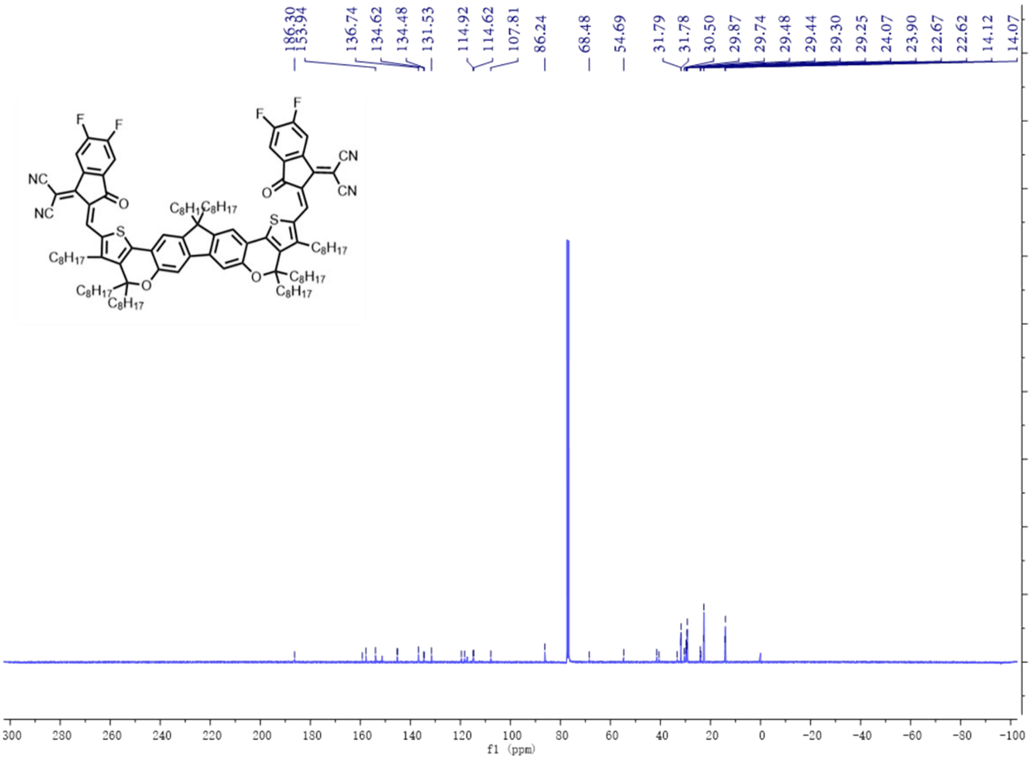

Fig. S20 ^{13}C NMR spectra of compound FOR-2F in $CHCl_3$

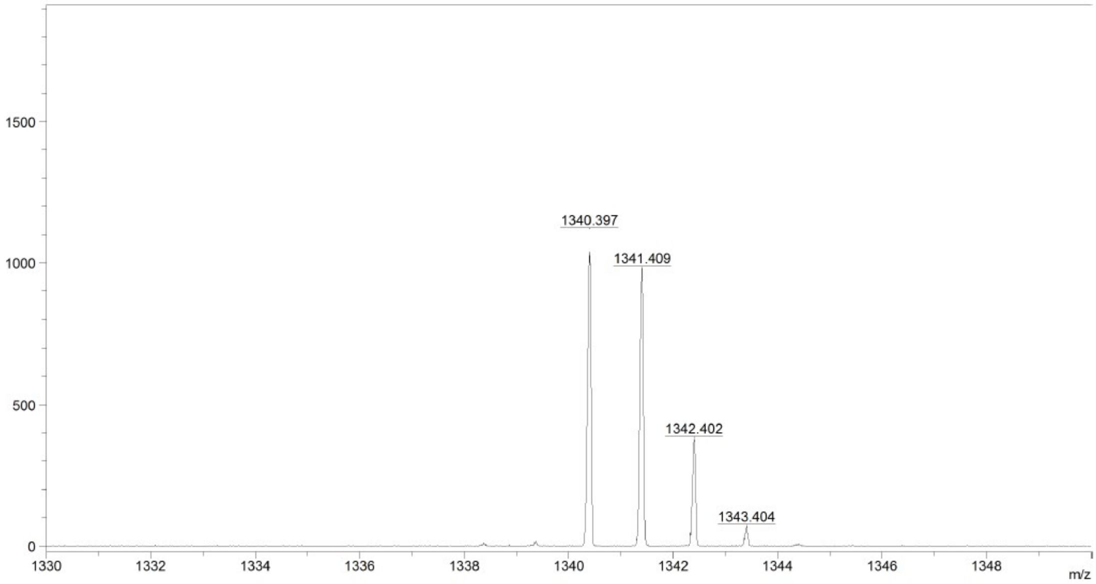

Fig. S21 HR-MS plots of Compound 10

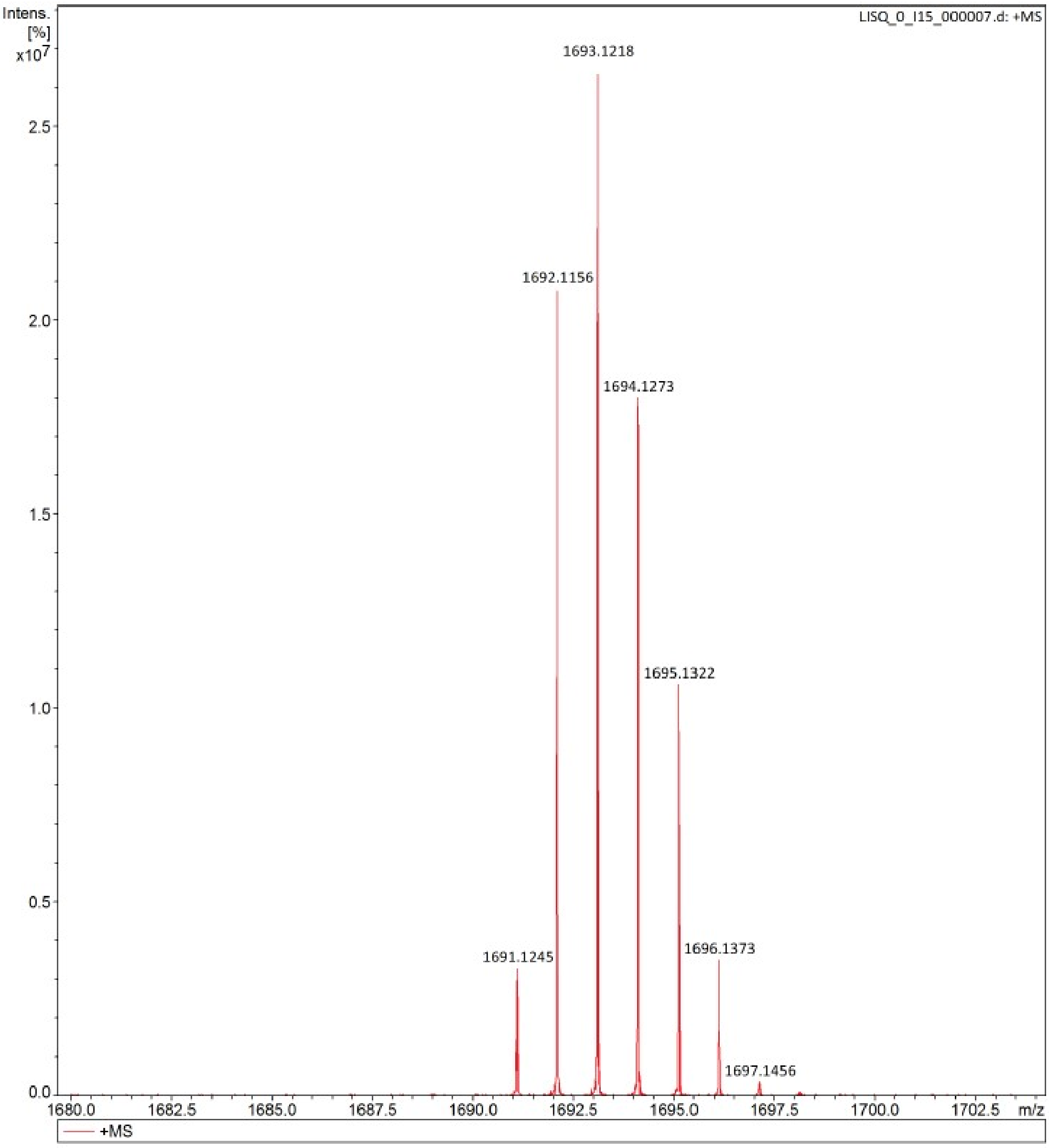

Fig. S22 HR-MS plots of compound FOR-IN

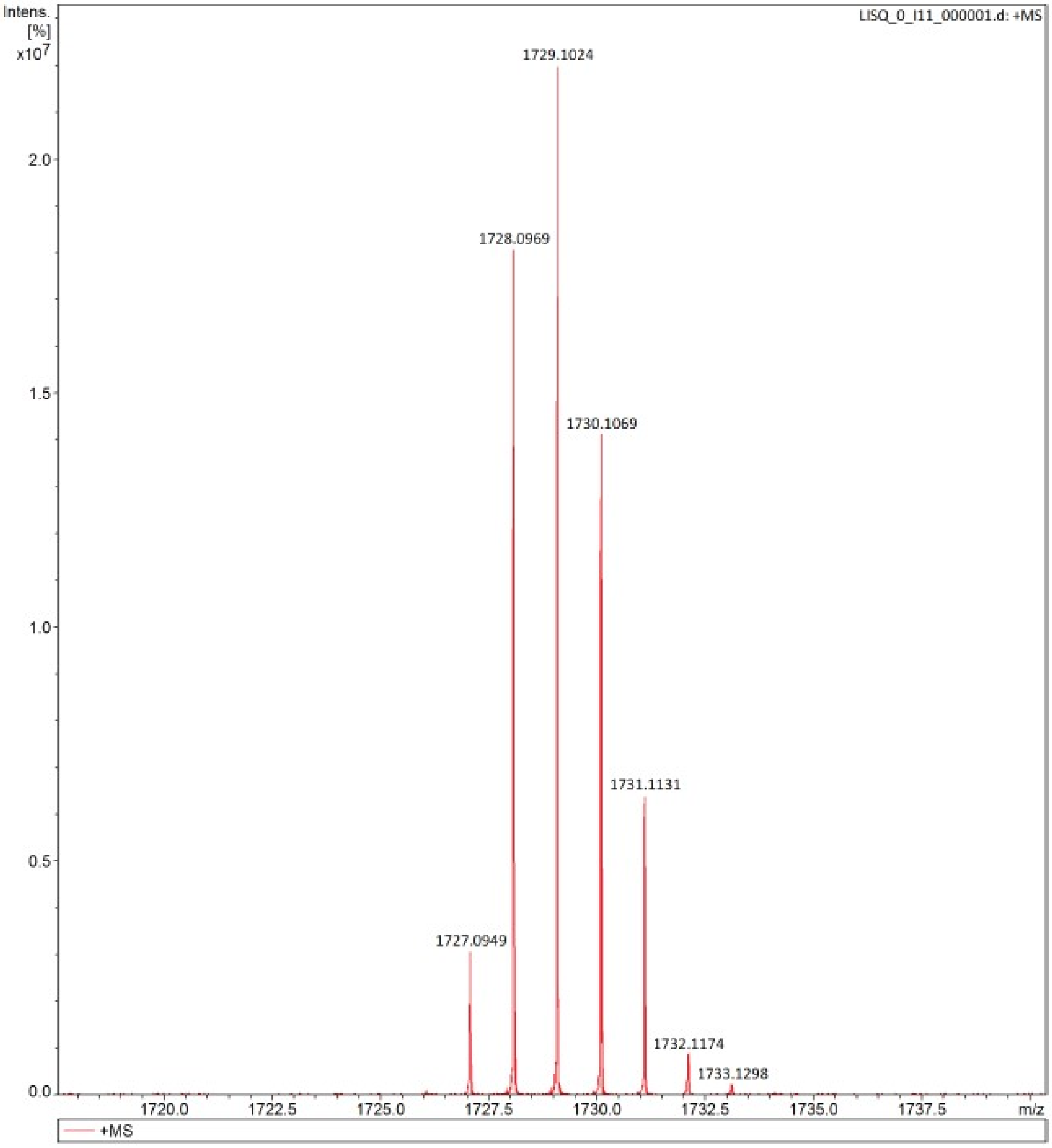

Fig. S23 HR-MS plots of compound FOR-1F

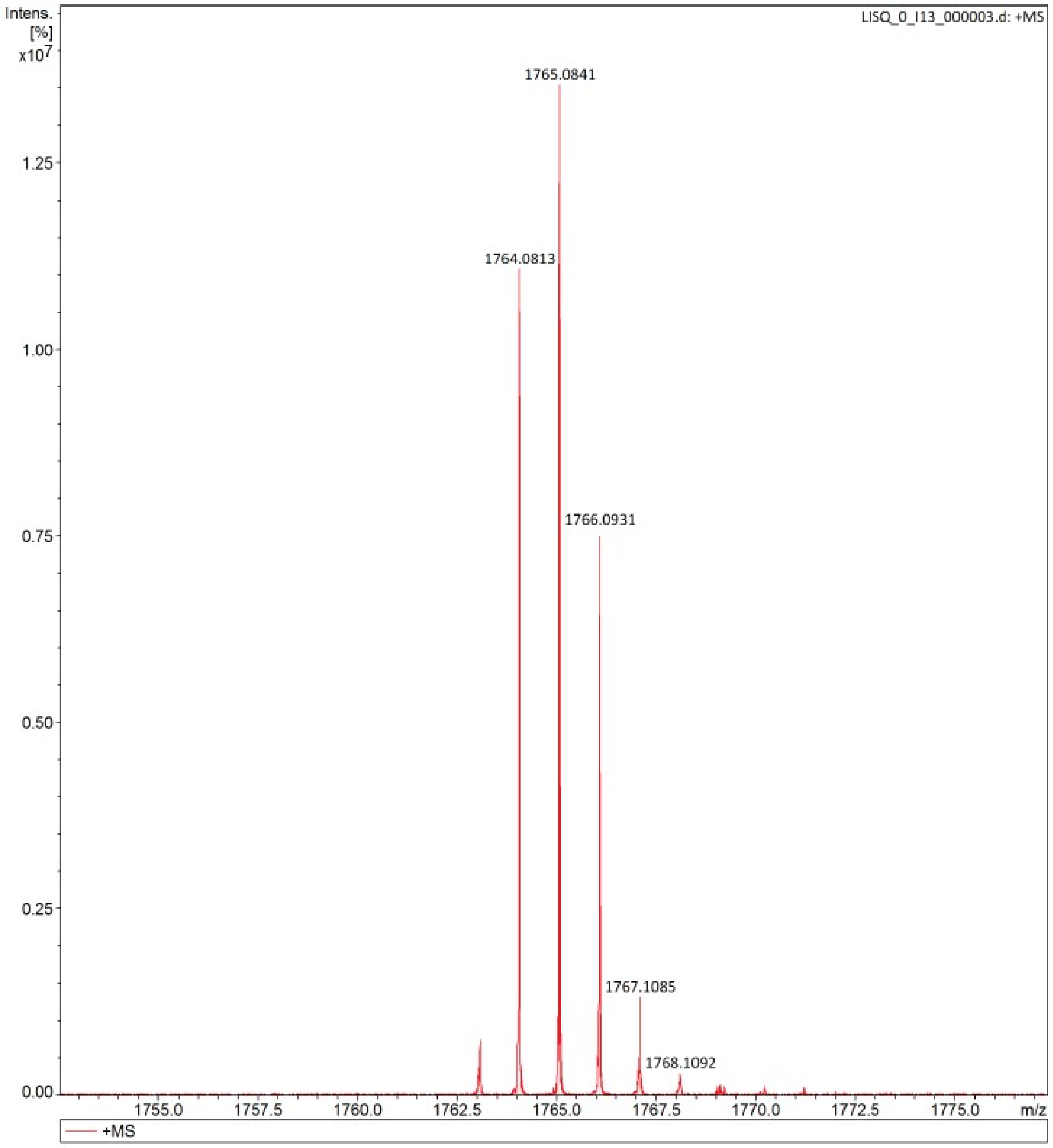

Fig. S24 HR-MS plots of compound FOR-2F

References

1 H. G. Kim, M. Kim, J. A. Clement, J. Lee, J. Shin, H. Hwang, D. H. Sin and K. Cho, *Chem. Mater.*, 2015, **27**, 6858-6868.

2 X. Ke, L. Meng, X. Wan, M. Li, Y. Sun, Z. Guo, S. Wu, H. Zhang, C. Li and Y. Chen, *J. Mater. Chem. A*, 2020, **8**, 9726-9732.